Natural Product Reports

ROYAL SOCIETY OF CHEMISTRY

REVIEW

View Article Online
View Journal

Cite this: DOI: 10.1039/d6np00030d

The elansolids: how nature shows chemists how to tame *p*-quinone methides

Liang-Liang Wang, *[a] Xiao-Qin Zhou[ab] and Andreas Kirschning *[cd]

Covering: up to 2025

Elansolids are metabolites isolated from the gliding bacterium *Chitinophaga sancti* (formerly *Flexibacter* spec.). The fascinating structures of this type of natural products, as well as their promising biological antibiotic activities, have triggered considerable efforts in the study of elansolids, especially their biosynthesis, which features the formation of highly reactive *p*-quinone methide intermediates in the enzymatic dehydration-IMDA process. This review focuses on the various aspects of *p*-quinone methides, including their formation, reactivities (chemical transformations), and applications in total synthesis, all of which are elucidated based on the example of elansolids. By highlighting this particular instance of *p*-quinone methides, it is shown how nature, namely, the enzymes in the PKS assembly line, could tame this type of highly reactive intermediate. Furthermore, by mimicking the *p*-quinone methide-mediated IMDA process as observed in biosynthesis, chemists can rationally access various synthetically challenging intermediates, for instance tetrahydroindanes, and utilize them in the total synthesis of the elansolid family.

Received 21st March 2026

DOI: 10.1039/d6np00030d

rsc.li/npr

[a]*State Key Laboratory of Phytochemistry and Natural Medicines, Kunming Institute of Botany, Chinese Academy of Sciences, Kunming 650201, People's Republic of China. E-mail: wangliangliang@mail.kib.ac.cn*

[b]*University of Chinese Academy of Sciences, 100049, Beijing, PR China*

[c]*Institute of Organic Chemistry, Leibniz Universität Hannover, Schneiderberg 1B, 30167 Hannover, Germany. E-mail: andreas.kirschning@oci.uni-hannover.de*

[d]*Uppsala Biomedical Center (BMC), Uppsala University, Husargatan 3, 752 37 Uppsala, Sweden*

1. Introduction

1.1 Quinone methides in nature

Quinone methides are the C-analogs of quinones in which one carbonyl group is replaced by methylene. Accordingly, *para*- and *ortho*-quinone methides **1a** and **b** are known.[1] They are regarded as cross-conjugated rather than aromatic systems and exhibit strongly electrophilic properties because the Michael-type radical or nucleophilic addition to the exocyclic double bond is a very facile process by which the aromaticity is recovered.[2]

Simple, unhindered quinone methides are highly reactive and are known only as short-lived intermediates that trimerize under normal conditions in the absence of nucleophiles.[3] Nature has also encountered this unusual functional group, as documented in several natural products,[4] such as in bioactive triterpenoids, for instance, celastrol and pristimerin (**2a** and **b**),[5] 20-*epi*-isoiguesterinol (**3**),[6] amazoquinone (**4**),[7] tingenone (**5**) and netzahualcoyonol (**6**),[8] taxodone (**7**) and its oxidation product taxodione (**8**),[9] as well as the polyketides kendomycin (**9**)[10] and elansolid A3 (**10**),[11] just to name some typical examples. Generally, the quinone methide group present in several natural products, specifically in diterpenoids **7** and **8**, isolated from *Taxodium distichum* (bald cypress), *Rosmarinus officinalis* (rosemary) and several *Salvia* species, is responsible for their anticancer,[9,12] antioxidant,[13] and other biological activities.[14]

Oxidation to a reactive quinone methide is the mechanistic basis of many phenolic anti-cancer drugs.[15] Often the phenol is

first oxidised to catechol **11**, further oxidised to *o*-quinone **12**, and finally isomerised to *p*-quinone methide **13**. This then serves as a Michael acceptor for nucleophiles, and driven by re-aromatisation, catechol **14** is formed again, which is now functionalised in the benzyl position (Scheme 1B).[1f,4,16] In addition, *p*-quinone methides can be biosynthetically produced *via* two other routes. This is achieved either by enzymatic oxidation of *p*-substituted phenol **15** or by elimination of *p*-substituted phenol **16** functionalised in the benzyl position with a potential leaving group, and this can be traced back biosynthetically to the corresponding starting phenol.[1g,4,16]

Among the natural products listed in Scheme 1A, one *p*-quinone methide stands out, namely, elansolid A3 (**10**), because of the presence of the exocyclic C=C double bond in the *p*-quinone methide unit, which is not part of a second ring.[11] It seems remarkable that elansolid A3 could be isolated at all and not the corresponding 1,6-addition product formed by a biological nucleophile present in the fermentation broth or even with water, although the methide unit is more exposed than in a cyclic environment. The unusual stability of elansolid A3 can presumably be attributed to the following factors: (1) the presence of the geminal methyl group in close spatial proximity to the quinone methide motif and the resulting preferred conformation, which orients the quinone methide unit at approximately 90° to the bicyclic ring system, shields one side of the π-system from nucleophiles. To a lesser extent, this also applies to the presence of the linear polyketide chain, which hinders the Michael addition of nucleophiles from the other β-face, albeit to a lesser degree. (2) The attachment of the quinone methide unit to the bicyclic tetrahydroindane system results in an additional sterically bulky environment, which minimises the tendency towards trimerisation. (3) Furthermore, the isolation conditions were strictly controlled and kept anhydrous. This allowed elansolid A3 to be protected from attack by water, at least during the isolation process. The fact that **10** could be isolated and fully characterised led to speculations about the possible biosynthesis of this unusual type 1 polyketide, allowing the development of concepts for a biomimetic strategy for a total synthesis.

This overview focuses on the comprehensive studies conducted with elansolid A3 (**10**) and *p*-quinone methide intermediates, ranging from its biosynthesis, *via* its unique inherent reactivity, to total synthesis applications. Overall, this should contribute to a deeper understanding of *p*-quinone methides, not only from a chemical point of view, but especially with regard to the question of how nature manages to exploit and control this remarkable reactivity. These topics are summarised in this article with the intention of providing another telling

Liang-Liang Wang

Liang-Liang Wang obtained his Bachelor's degree from Anhui University, China, in 2003, and his PhD degree from the Chengdu Institute of Organic Chemistry, the Chinese Academy of Sciences (CAS), in 2012. He then continued as a postdoctoral fellow under Prof. Fabien Gagosz at the École Polytechnique in France, and later under Prof. Andreas Kirschning at the Leibniz University Hannover in Germany, where he worked on the synthesis of natural products. In 2017, he joined the Kunming Institute of Botany (KIB), CAS, as an associate professor. He is currently a professor. His laboratory focuses on the total synthesis and medicinal chemistry of natural products.

Xiao-Qin Zhou

Xiao-Qin Zhou was born in Guizhou, China. She completed her Bachelor's degree at the Guizhou Medical University in 2020. After graduation, she moved to the Kunming Institute of Botany (KIB), CAS, where she joined Prof. Liang-Liang Wang's laboratory to complete her Master's degree. Currently, her research focuses mainly on the synthesis of natural products.

Andreas Kirschning

Andreas Kirschning received his PhD degree at the University of Hamburg in 1989 under the guidance of Prof. E. Schaumann. After a postdoctoral stay with Prof. Heinz G. Floss in the USA, he moved to the Technical University of Clausthal and completed his habilitation. In 2000, he became a full professor at the Leibniz University of Hannover, and since 2024, he has been co-affiliated with the Uppsala University (Sweden). His research interests include all aspects of natural products, including total synthesis, mutasynthesis and terpene synthases. Another area of his research, first published in 2001, covers flow chemistry and enabling technologies in organic synthesis, such as inductive heating. Recently, his interest expanded to theoretical aspects of molecular evolution and the origin of life, with a focus on the role of coenzymes and cofactors.

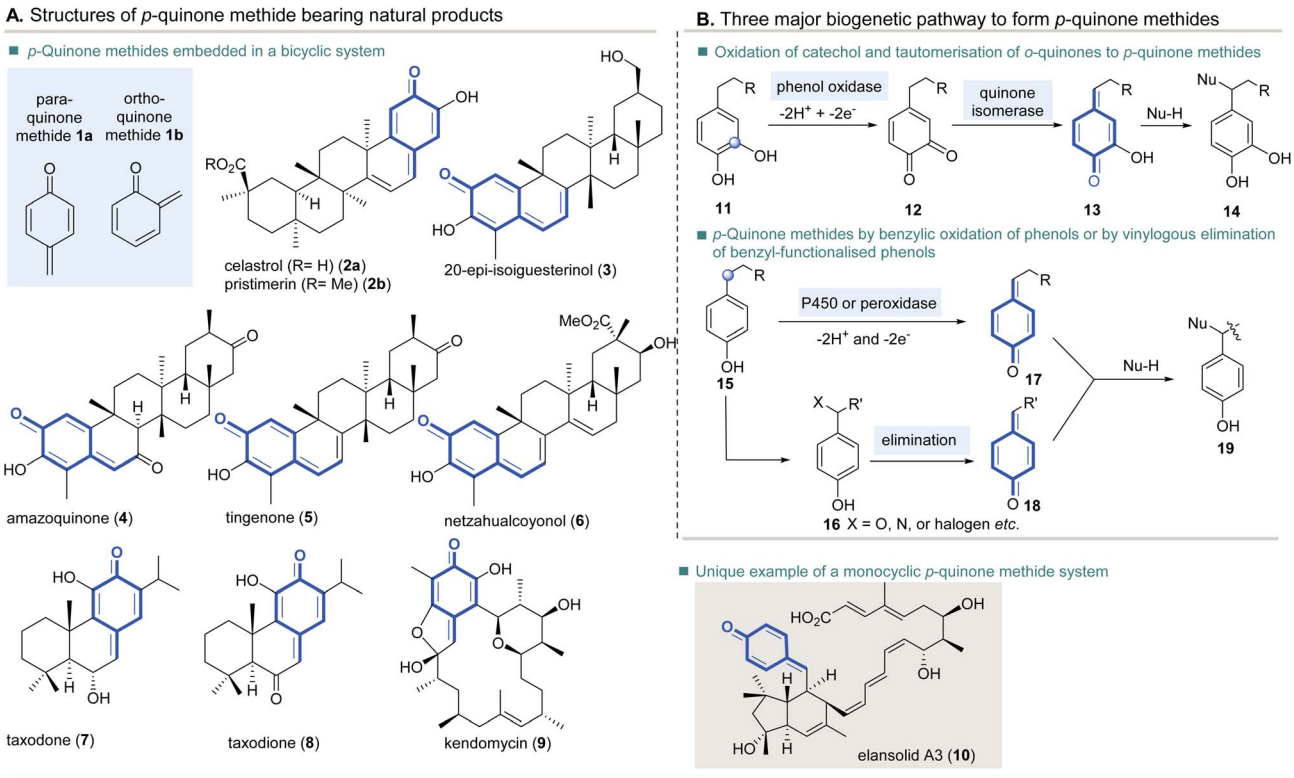

Scheme 1 (A) Principal structures of *p*- and *o*-quinone methides and the structures of selected natural products **2**–**10** that bear these subunits. (B) Enzymatic formation of the *p*-quinone methides **13**, **17** and **18**. Commonly, these undergo 1,6-additions with nucleophiles or radicals.

example that nature can be a blueprint for synthetic organic chemistry.

2. Investigations on the extraordinary properties of the *p*-quinone methide elansolid A3

2.1 Isolation, structure elucidation, and bioactivity

Elansolid A1 (**20**) and its atropisomer elansolid A2 (**20***) belong to a larger group of polyketides first isolated from the gliding bacterium *Chitinophaga sancti* (formerly *Flexibacter* spec.).[17,18] A closer inspection revealed that the extracts also contained elansolid B1 (**21a**), B2 (**21b**), B3 (**21c**), D1 (**22**), and D2 (**23**) (Fig. 1).[19,20] Elansolid A3 (**10**) proved to be a remarkable new derivative that could only be isolated under strictly controlled and anhydrous conditions. It contains a *p*-quinone methide unit and is not only structurally unique, but also provides insights into the underlying biosynthesis with key steps for the entire class of elansolids.[11]

It was assumed that the macrocyclic atropisomers A1/A2 (**20**/**20***) form through spontaneous, non-enzymatic addition of the carboxyl group to the quinone methide unit in elansolid A3 (**10**). This special reactivity may also explain the formation of elansolids B1–B3 (**21a–c**), which are thought to be artefacts resulting from nucleophilic attack by water, methanol or ammonia, during the post-fermentation workup process.[11,19]

The structure elucidation of elansolids A1/A2 (**20**/**20***) was based on several strategies: (A) NMR spectroscopic analysis including nOe assignments, (B) acetonide formation and analysis using Rychnowski's method,[21,22] and (C) chemical degradation *via* cross-metathesis using ethylene as an external alkene to yield fragments **24** and **25**.[23] This was accompanied by the total synthesis of the C1–C11 fragment **25** and comparison of

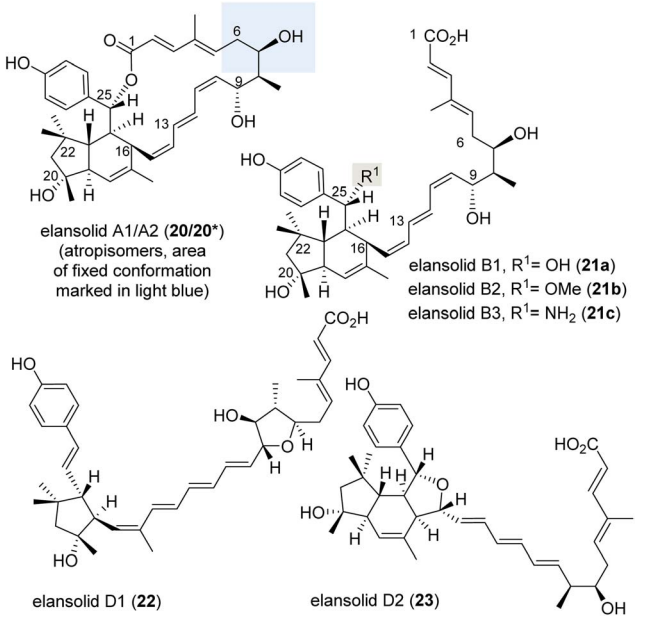

Fig. 1 Elansolid family of polyketides (structure of elansolid A3 (**10**) shown in Scheme 1).

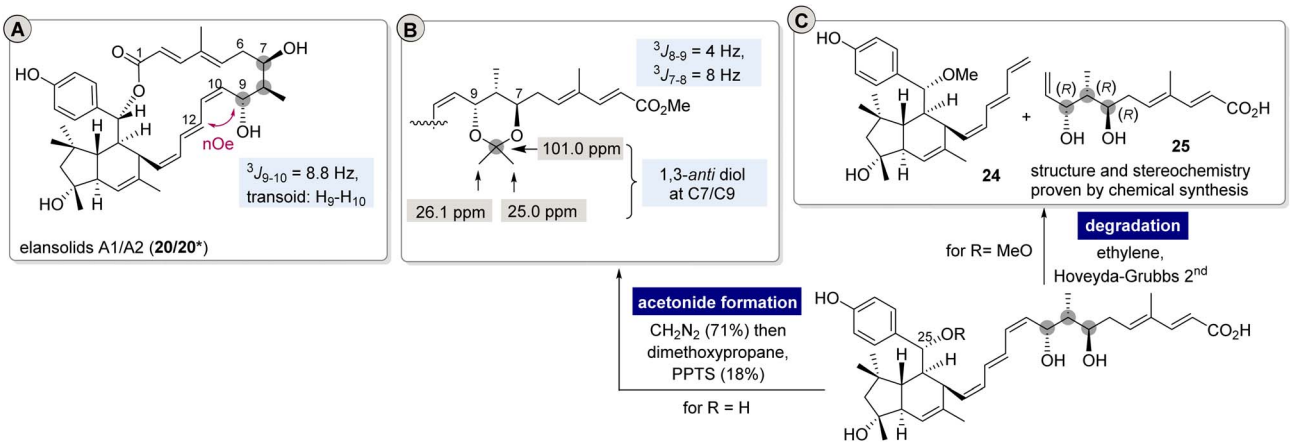

Scheme 2 Specific methods employed to elucidate the structure of elansolid A1/A2 (**20**/**20***). (A) NMR spectroscopic analysis of elansolid A1/A2 (**20**/**20***); (B) structural analysis using Rychnowski's method; (C) chemical degradation using cross-metathesis using ethylene as external alkene.

spectroscopic data and the optical rotation with the data collected from the metathesis fragmentation (Scheme 2).[18]

In particular, the last approach allowed the determination of both the relative and the absolute configurations of all three stereogenic centers at C7–C9 in elansolids A1/A2 (**20**/**20***). Consequently, the configurations in the stereotriad of seco acids **21a** and **21b**, as well as tetrahydrofurans **22** and **23**, are alike (7*R*, 8*R*, 9*R*). Furthermore, molecular modeling calculations revealed that the conformational differences between the two atropisomers, **20** and **20***, are ascribed to the different orientations of the backbone element at C6/C7.[18] C6 in the former atropisomer elansolid A1 (**20**) is "folded out" of the lactone ring, while the secondary alcohol C7 is "folded inwards" into the lactone ring. In the case of elansolid A2 (**20***), the methylene group C6 adopts a "folded in" conformation, while the alcohol at C7 is directed outwards.

The chemical reactivity of the *p*-quinone methide unit and the chemical relationship of the elansolids could be verified

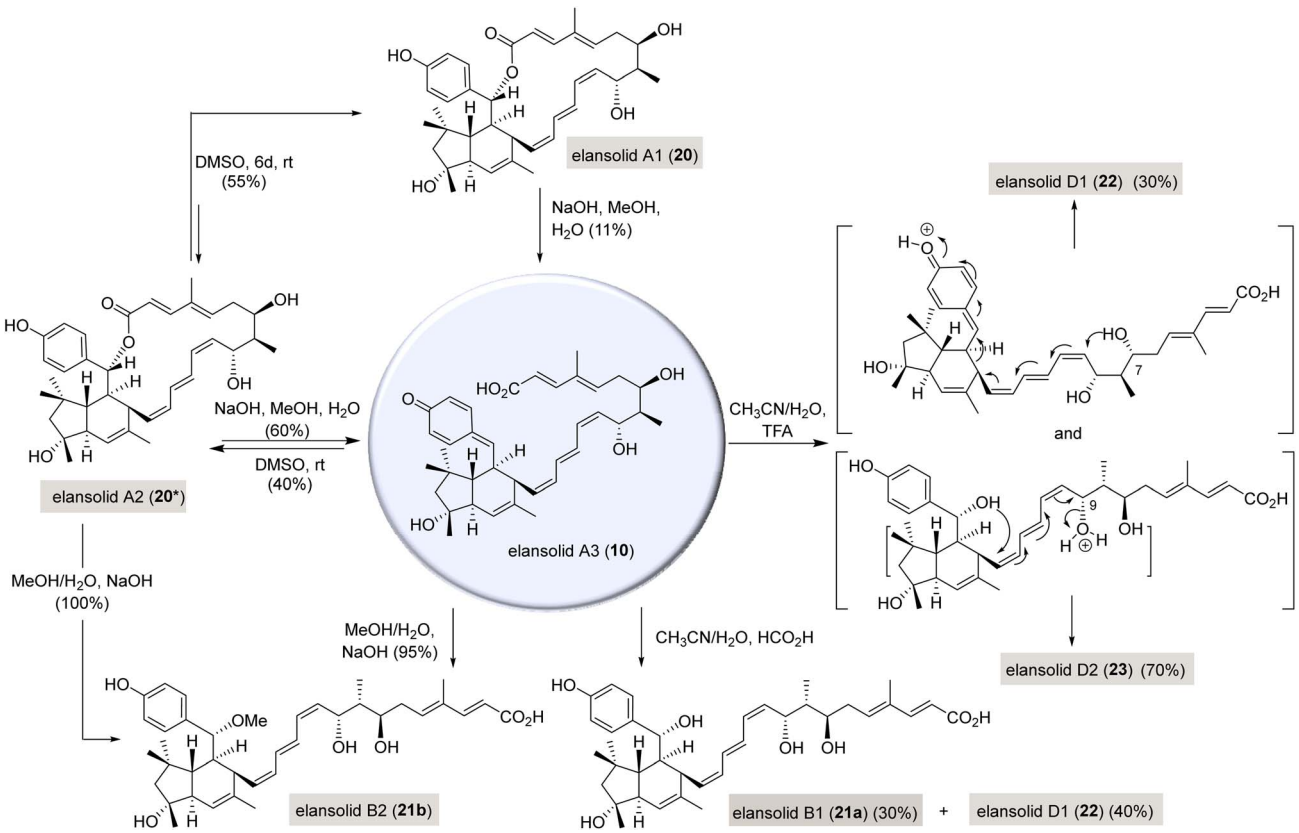

Scheme 3 Chemical conversions of the quinone methide **10** into its related natural products.

chemically, starting from elansolid A3 (**10**) as summarised in Scheme 3.[11] Elansolid A3 (**10**) spontaneously converts to the macrocyclic elansolid A2 (**20***) in DMSO without the need for a basic or acidic activator. Under these conditions, macrolactonisation is dynamically favoured. With longer reaction times (6d in DMSO), the atropisomer elansolid A2 (**20***) could be converted into elansolid A1 (**20**). This observation underscores that the latter conformer is thermodynamically favoured. Consequently, both atropisomers elansolid A2 (**20***) and A1 (**20**) could be reversibly converted back into elansolid A3 (**10**) under basic conditions. In a diluted solution (0.1 M) of NaOH in methanol, Michael addition of elansolid A3 (**10**) predominantly forms elansolid B2 (**21b**). Under these conditions, elansolid B2 is also formed directly from the macrolide elansolid A2 (**20***).

In contrast, under aqueous acidic conditions (HCO_2H), water is added directly to elansolid A3 (**10**), resulting in elansolid B1 (**21a**), but elansolid D1 (**22**) is also formed under these conditions. When a stronger acid such as trifluoroacetic acid (TFA) is employed, the allyl alcohol at C9 in **21a** becomes activated and elimination is initiated, leading to the formation of the tetrahydrofuran-containing elansolid D2 (**23**) *via* a vinylogous cyclisation. In addition, elansolid D1 (**22**) is found as a by-product, which is formed by an oxacyclisation coupled with a Grob fragmentation.

With this knowledge in hand, precursor-directed biosynthesis[24] allowed the generation of new elansolid derivatives. This was achieved by adding external nucleophiles to the crude extracts collected after the fermentation, which reacted with elansolid A3 (**10**) present in the broth, yielding 22 new derivatives overall, of which selected examples **26–29** are listed in Table 1.[19,25] It should be noted that in all cases, only the (25*R*) diastereomer was formed, as is the case with elansolids **20**/**20***, **21a–c** and **23**. The synthetically produced tetrahydroindane derivative **30** served as a model to gain insights into the observed diastereoselectivity. It was shown that, in terms of conformation, the *p*-quinone methide plane of **30** is aligned at a 90° angle to the bicyclic system, which leads to shielding of the (*si*)-face by the geminal methyl groups. Consequently, the (*re*)-face is preferentially accessible to nucleophiles.

The elansolids exhibit antimicrobial activity against gram-positive bacteria, including *M. luteus* and *S. aureus*. Elansolid A3 also exhibits a promising antibiotic profile against these bacteria with an MIC in the range of 0.2–64 μg ml^{-1}; however, it is unclear whether the effect can actually be attributed to this derivative, since another derivative may well be responsible for the biological activity after the addition of a nucleophile from the test system.[11] This is because elansolid A2 (**20***) exhibits a very similar antibiotic effect to elansolid A3 (**10**). In contrast, its atropisomer elansolid A1 (**20**) is less active.[18] From these observations, it can be inferred that the hydroxyl group at C7 likely plays an important role in determining the antibiotic profile. This is because the structural difference between elansolid A1 (**20**) and A2 (**20***) is based on the "folded-in"/"unfolded" conformation around the C6–C7 bond.

The synthetic derivative 20-deoxy-elansolid (**31**) with an open macrocycle exhibits similar inhibitory effects against various gram-positive strains, suggesting that the hydroxyl group at position 20 is not essential for maintaining the antibacterial

Table 1 Minimum inhibitory concentrations (MICs) of the elansolids **10** and **20**/**20*** and their derivatives **26–29** collected by precursor-directed biosynthesis against *Micrococcus luteus* and *Staphylococcus aureus* MRS 3

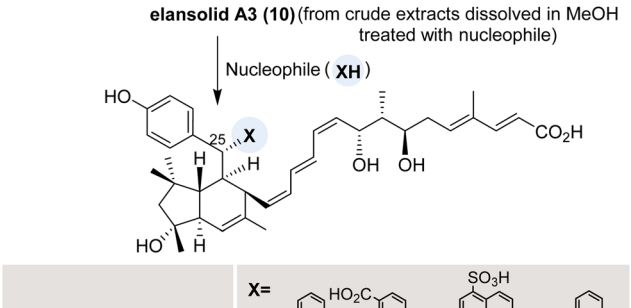

MIC [μg/mL]	20	20*	10	26	27	28	29
M. luteus	8.3	0.3	0.3	0.5	0.5	0.5	0.5
S. aureus	33	7.2	7.2	8.3	8.3	8.3	8.3

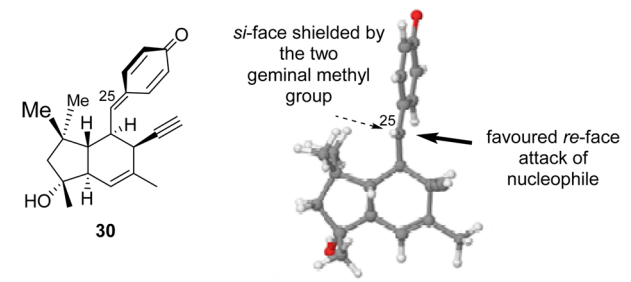

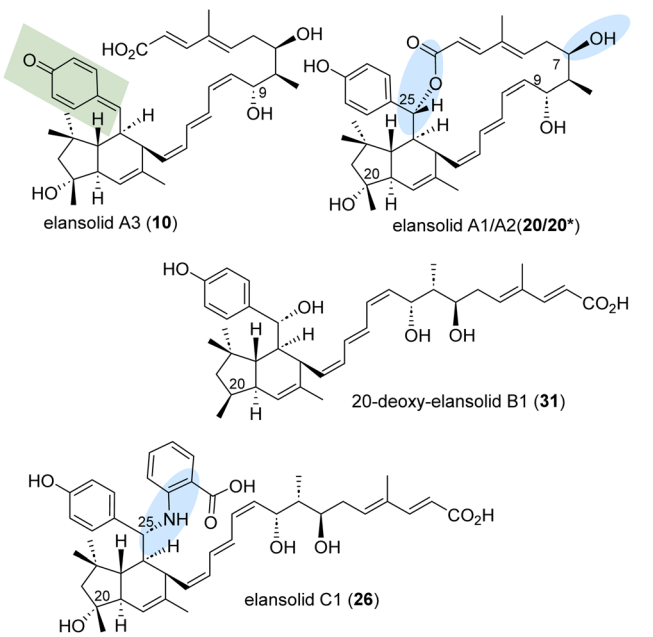

Fig. 2 Preliminary considerations of pharmacophoric elements in elansolids essential for the antibacterial activity (highlighted in blue) and cytotoxicity against L929 cells (highlighted in green).

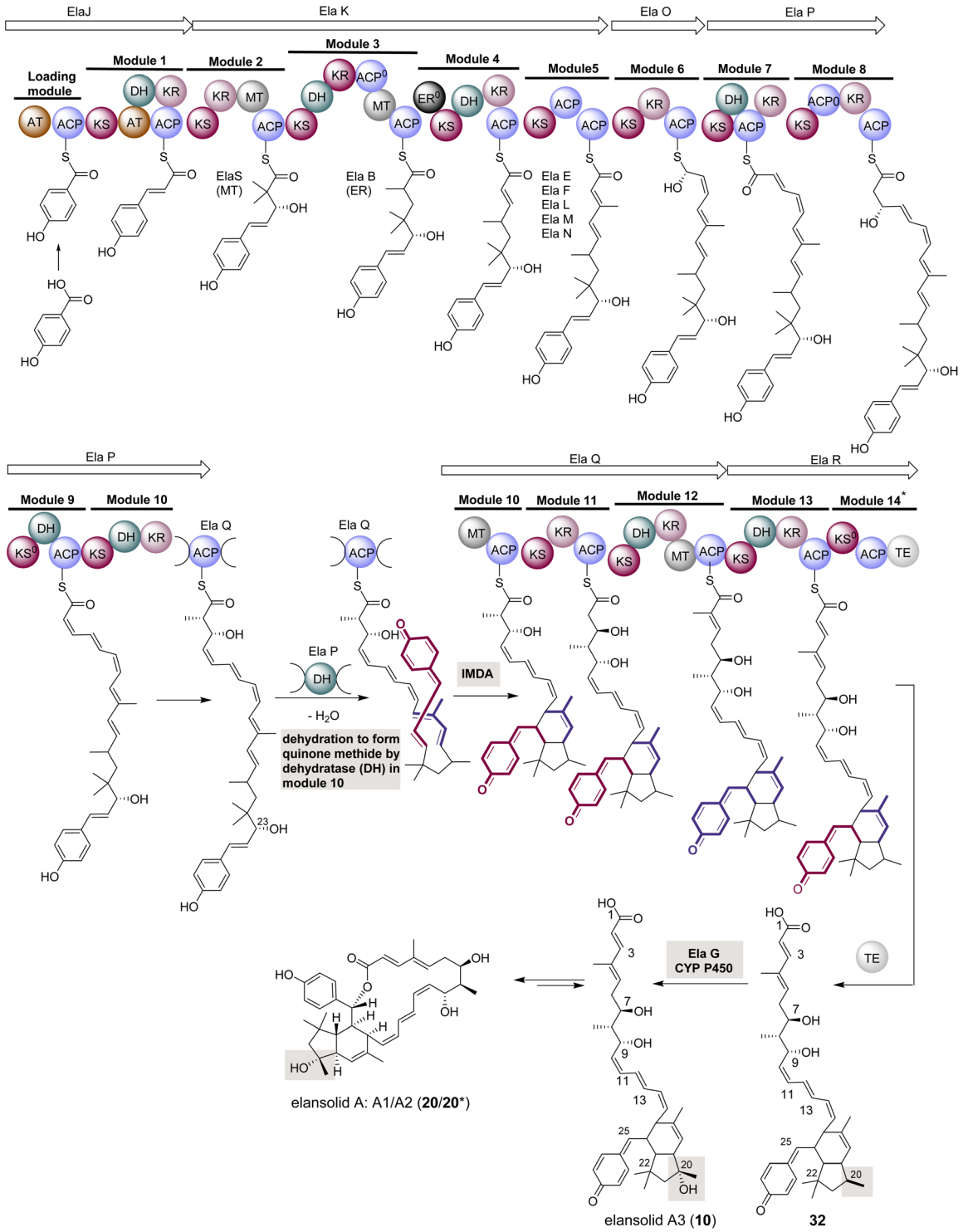

Scheme 4 Proposed biosynthesis pathway of elansolid A3 (**10**) based on the feeding experiment with ^{13}C-labeled precursors and analysis of the gene locus in *Chitinophaga sancti*.

profile of elansolids.[26] The derivatives (**26–29**) obtained *via* precursor-directed biosynthesis, which carry a bulky substituent at C25, exhibit antibiotic activity comparable to that of elansolid A2 (**20***).[19] These cases suggest that a substitution at C25 by a bulky group, or the presence of a conformationally rigid macrolactone ring, is likely conducive to the maintenance of antibiotic activity.

In addition to its antibacterial activity, elansolid A3 exhibits cytotoxicity against L929 mouse fibroblast cells with an IC_{50} value of 12 mg ml^{-1}.[11] In contrast, the macrolactone elansolid A2 (**20***) exhibits lower toxicity (IC_{50} = 33 mg ml^{-1}), and

elansolid A1 (**20**) appears to be non-toxic (up to 40 mg ml^{-1}).[19] The quinone group in elansolid A3 is likely responsible for this cytotoxicity due to its pronounced chemical reactivity (Fig. 2).

2.2 Biogenetic formation of *p*-quinone methide and related natural products

The discovery of elansolid A3 (**10**) paved the way for the development of a comprehensive biosynthesis model with the *p*-quinone methide unit as the central playground, which should be universally applicable to all elansolids.[27] Sequencing and analysis of the biosynthetic gene cluster suggested that the PKS responsible for the formation of elansolid A3 is a *trans*-AT synthase, and its architecture is given in Scheme 4.[27,28] Feeding experiments with ^{13}C-labeled precursors revealed that *p*-hydroxybenzoic acid serves as the starting building block. Overall, processing along 14 PKS modules provides the C20-deoxy-seco acid of elansolid A3 (**32**) after hydrolytic cleavage from the PKS on the stage of the thioesterase (TE) domain. The formation of the tetrahydroindane core was suggested to occur in the dehydratase (DH) domain of module **10**. Dehydration at position C23 would yield the vinylic quinone methide, which is ideally positioned to induce an IMDA cycloaddition.

The biosynthesis is terminated by a tailoring oxidation at C20, which introduces the tertiary hydroxy group, yielding elansolid A3 (**10**), which then leads to the atropisomers **20**/**20*** after an intramolecular Michael addition. However, it is difficult to pinpoint the exact timing of a cycloaddition within the biosynthetic assembly line, as is the case here. One reason for this is that Diels–Alderases do not necessarily trigger the cycloaddition but that other enzymes could also catalyse the step prior to cyclisation. These include dehydratases or alcohol dehydrogenases, which, *e.g.*, supply the dienophile with an energetically lowered LUMO. The IMDA cycloaddition is then strongly triggered by the inherent chemical reactivity of the functional groups and thus proceeds spontaneously.[29]

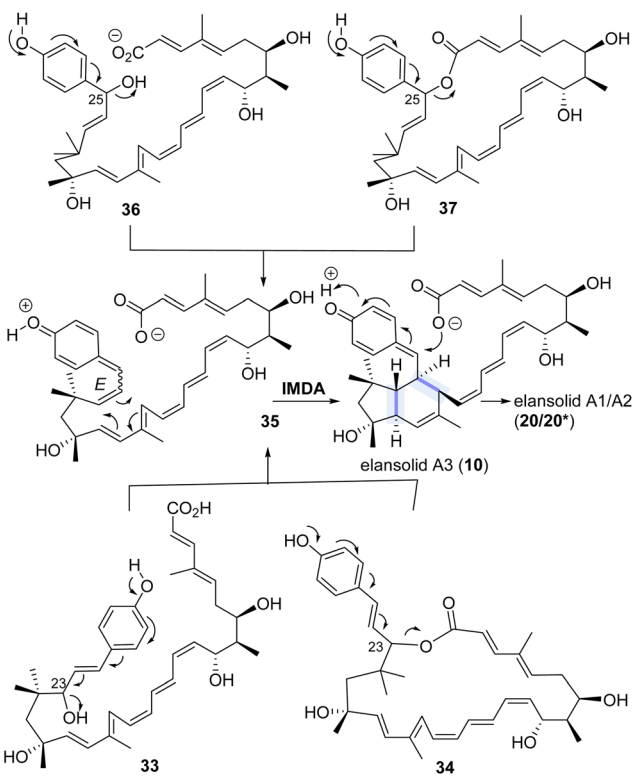

Scheme 5 Biosynthetic considerations for the IMDA cycloaddition starting from open-chain and macrocyclic precursors after the cleavage of the PKS chain.

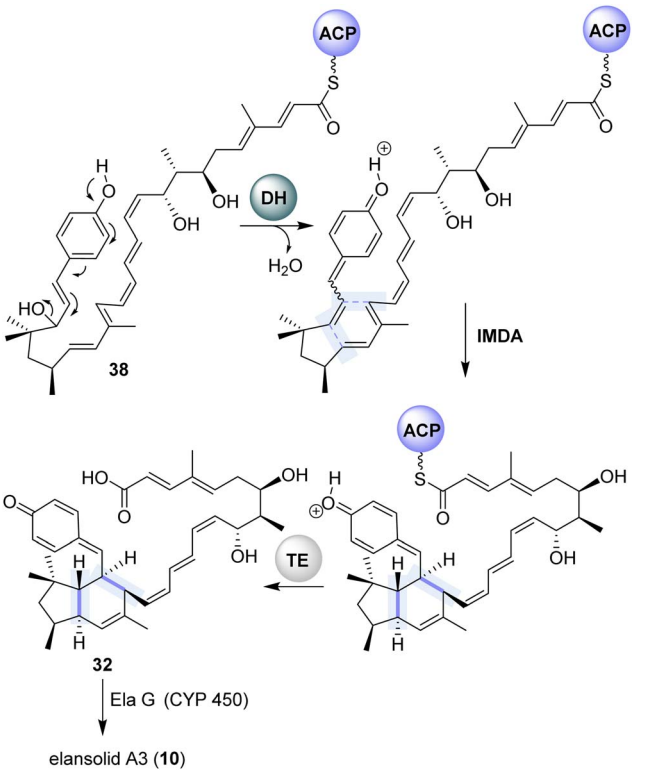

Scheme 6 Proposed IMDA reaction occurring at the late stage of the PKS assembly line.

Apart from the case shown in Scheme 4, it cannot be ruled out that the linear PKS chain continues to elongate without the occurrence of an IMDA reaction, ultimately leading to C23-allylic compound **33** or C23-macrolactone **34**. These are formed following a thioesterase-promoted cleavage from the PKS (Scheme 5). These two intermediates thus tend to undergo dehydration, yielding the quinone methide **35**, which subsequently undergoes IMDA cyclisation to yield elansolid A3 (**10**).[27] From a chemical perspective, C25-benzyl alcohol **36** and C25-macrolactone **37** have also been discussed as potential substrates for this dehydration and cyclisation cascade. However, according to the biosynthesis shown in Scheme 4, the latter two intermediates are less likely candidates. The synthetic model studies in Schemes 7 and 8 below also support C23-allyl **33** or C23-macrolactone **34** and almost completely rule out C25-benzyl alcohol 36 and macrolactone **37** as precursors.

Alternatively, it could well be that the vinylogous dehydration that triggers the IMDA reaction may also take place at a later stage, namely, shortly before the hydrolytic cleavage by the TE, while still being attached to the PKS (Scheme 6).[30] After

the formation of the *p*-quinone methide, tailoring oxidation would finally take place at C20, resulting in elansolid A3 (**10**).

In order to clarify the precise timing of the dehydration and IMDA cycloaddition, it will therefore be necessary in the future to identify the possible enzymes that catalyse this cascade reaction—for example, the respective dehydratases in the PKS modules—and to validate the catalytic activity of these enzymes by adding suitable substrates. However, the chemical insights gained from the biosynthetic proposal serve as a guide for the total synthesis studies on the elansolids, which are discussed in detail in the following section.

3. Nature provided the idea for total synthesis approaches utilizing *p*-quinone methide chemistry

3.1 Model syntheses

The biosynthetic analysis and the chemical relationships between elansolid A3 (**10**) and the other elansolids described in Scheme 4 inspired the development of biomimetic total syntheses of these polyketides. To this end, model systems were first developed that replicate and mimic the cascade consisting of vinylogous dehydration, intramolecular Diels–Alder cycloaddition (IMDA), and the diastereocontrolled addition of a nucleophile to the *p*-quinone methide unit (Scheme 7).[27] Racemic tetrahydroindane **40** was collected by Brønsted acid-promoted activation of acetate **39**, proving the feasibility of the biosynthetic hypothesis, particularly with regard to the desired diastereocontrol in the IMDA cycloaddition, as well as the facial selectivity in the final capture of the nucleophile.

Based on this proof of principle, more complex precursor models **41–48** were designed in order to more closely mimic the proposed biosynthetic precursor **38** and to evaluate methods to develop an asymmetric version of this chemistry with *p*-quinone methides as key players.[30–32] The first generation of substrates **41** and **42** already contained the alcohol group at C20 in a protected form, a function that is only introduced biosynthetically after the IMDA. Both isomeric allyl alcohols (C23–C25) were probed. The second generation of IMDA precursors **43–45** corresponds more closely to the biosynthetic precursor **38** in terms of functionality at C20, as it is devoid of the hydroxyl group. Variations are based on different protective group patterns.[30] The drawback of these substrates is that it is impossible to selectively install the hydroxy group at a later stage by chemical means, which nature achieves with CYP450 monooxygenases. Importantly, the use of these substrates revealed that the effective implementation of IMDA depends heavily on the functionality at position C20 (see Scheme 8). The design of the third generation of substrates **46–48** builds on the IMDA results with the first two generations of substrates. These address the issues of the late-stage introduction of the hydroxy group and the challenge to achieve the preferred IMDA's facial selectivity. The hydroxyl group was preinstalled on the neighbouring carbon atom next to the stereogenic centre at C20 to enable oxidation at C20 after the IMDA cycloaddition.[31] In addition, a stereodirecting iodine atom was introduced at C18 of precursor **48** for a limited period of time in order to control the conformation of this substrate through induced 1,3-allyl strain. This conformational restriction was intended to enable high facial selectivity for IMDA cyclisation.[32]

3.2 Biomimetic IMDA cycloadditions

The two linear precursors **41** and **42** represent allylic regioisomers with the alcohol group either positioned at C23 or C25. Its protonation should therefore lead to the same *p*-quinone methide moiety and consequently, to the same cycloaddition

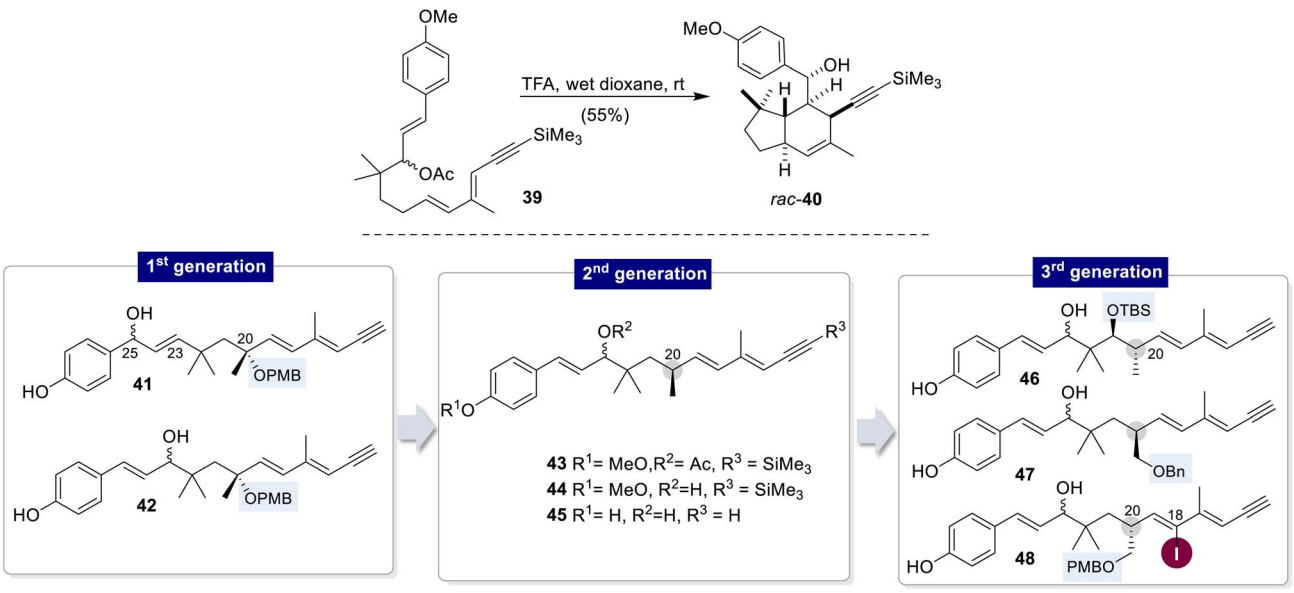

Scheme 7 (Top) preliminary reaction model **39** for testing the biomimetic IMDA reaction. (Bottom) design and evolution (1st to 3rd generation) of various substrates for exploring the biomimetic IMDA reactions (Ac = acyl, TFA = trifluoroacetic acid, PMB = *p*-methoxybenzyl, TBS = *tert*-butyldimethylsilyl, and Bn = benzyl).

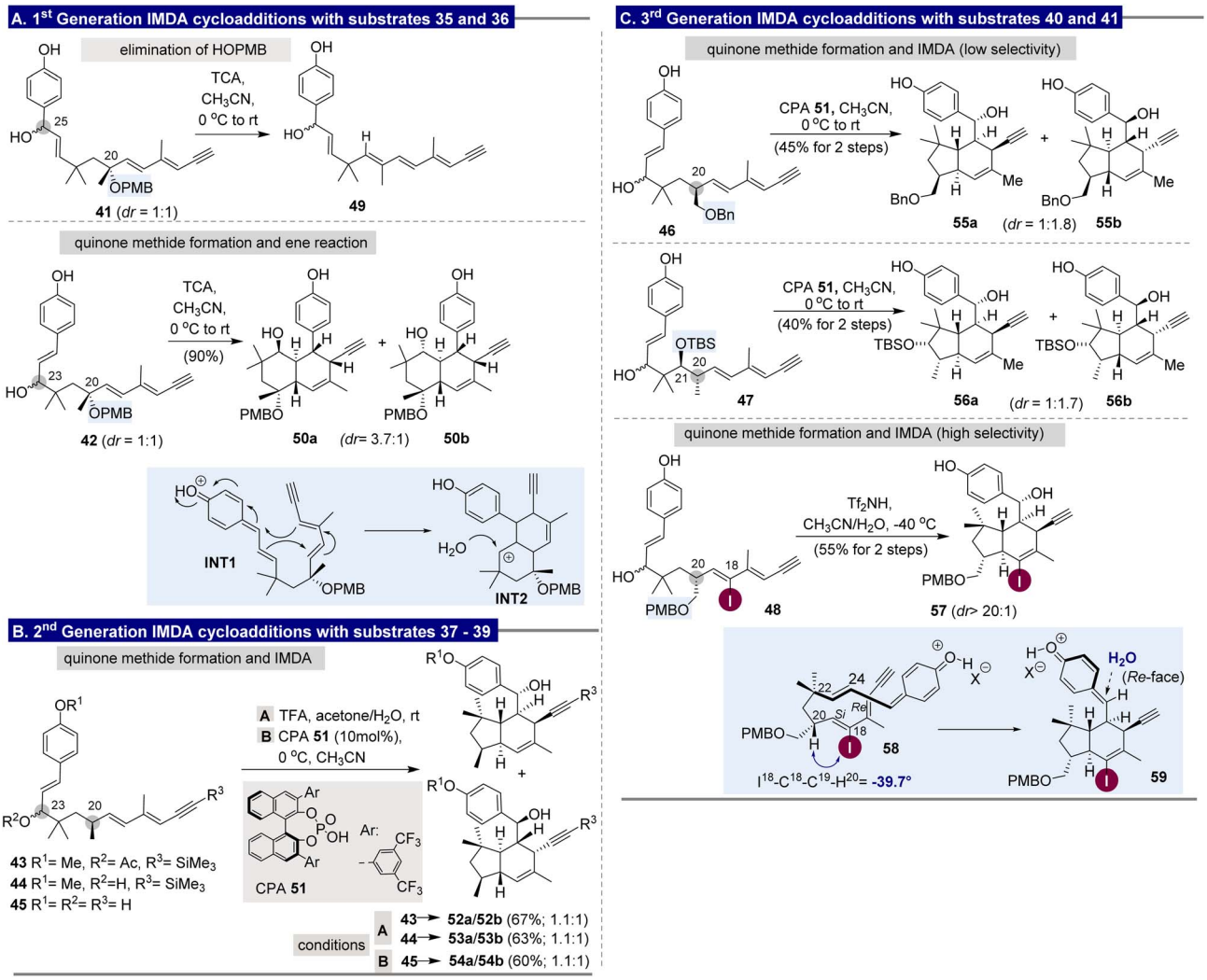

Scheme 8 Probing the biomimetic IMDA cycloadditions employing structurally diverse precursors **41–48**. (A) 1st generation IMDA cycloadditions with substrates **35** and **36**; (B) 2nd generation IMDA cycloadditions with substrates **37–39**; (C) 3rd generation IMDA cycloadditions with substrates **40** and **41** (TCA = trichloroacetic acid, CPA = chiral phosphoric acid, Tf = trifluoromethylsulfonyl).

product. None of the two precursors yielded any IMDA product. With **41**, only activation of the tertiary-bound OPMB group by TCA took place, which resulted in elimination to obtain the conjugated triene **49** (Scheme 8A).[29] In contrast, regioisomer **42**, which more closely resembles the putative biosynthetic intermediate **38**, yielded the two stereoisomeric products **50a** and **50b**. Instead of the desired tetrahydroindane skeleton, these contained the bicyclic octahydronaphthalene ring system. It was proposed that after the loss of water, the vinyl quinone methide **INT1** was formed. Instead of an IMDA reaction, a stepwise cascade ene-cyclisation must have occurred, which furnished carbocation **INT2**, and this was quenched by water to provide **50a** and **50b**. From these findings, it was concluded that the presence of tertiary carbinol at position 20 might be responsible for the occurrence of this stepwise process. The steric hindrance caused by this center would prevent the electrophilic vinyl quinone methide from approaching the diene unit to undergo the Diels–Alder cycloaddition. This may also shed light on the fact that the oxidation of C20 takes place as a biosynthetic tailoring step right after the IMDA reaction and not before. As a consequence, IMDA precursors **43–45**, lacking the oxyfunctionality at C20, were probed, which more closely mimic the biosynthetic intermediate **38** (Scheme 8B).[30] Either the Brønsted acid TFA or the chiral phosphoric acid (**51**) was able to smoothly form diastereomeric tetrahydroindanes **52a,b–54a,b**, but with poor selectivity (dr = 1.1 : 1). It is noteworthy that both the free secondary alcohol and its acetate at position **23** can be activated to form the vinylogous quinone methide intermediate that initiates the desired IMDA, just as has been proposed for the biosynthesis of elansolids.

The next generation of precursor substrates, therefore, did not contain a tertiary carbinol group at C20. In addition, a concept was developed to increase the facial selectivity of the IMDA process. Benzyl ether **46**, which was considered a suitable candidate for introducing the hydroxyl group at C20 after the IMDA, provided the cycloaddition products **55a** and **55b**, but with inadequate diastereocontrol (Scheme 8C, top right).[31] Precursor **47**, bearing an oxygen at C21, turned out to be also

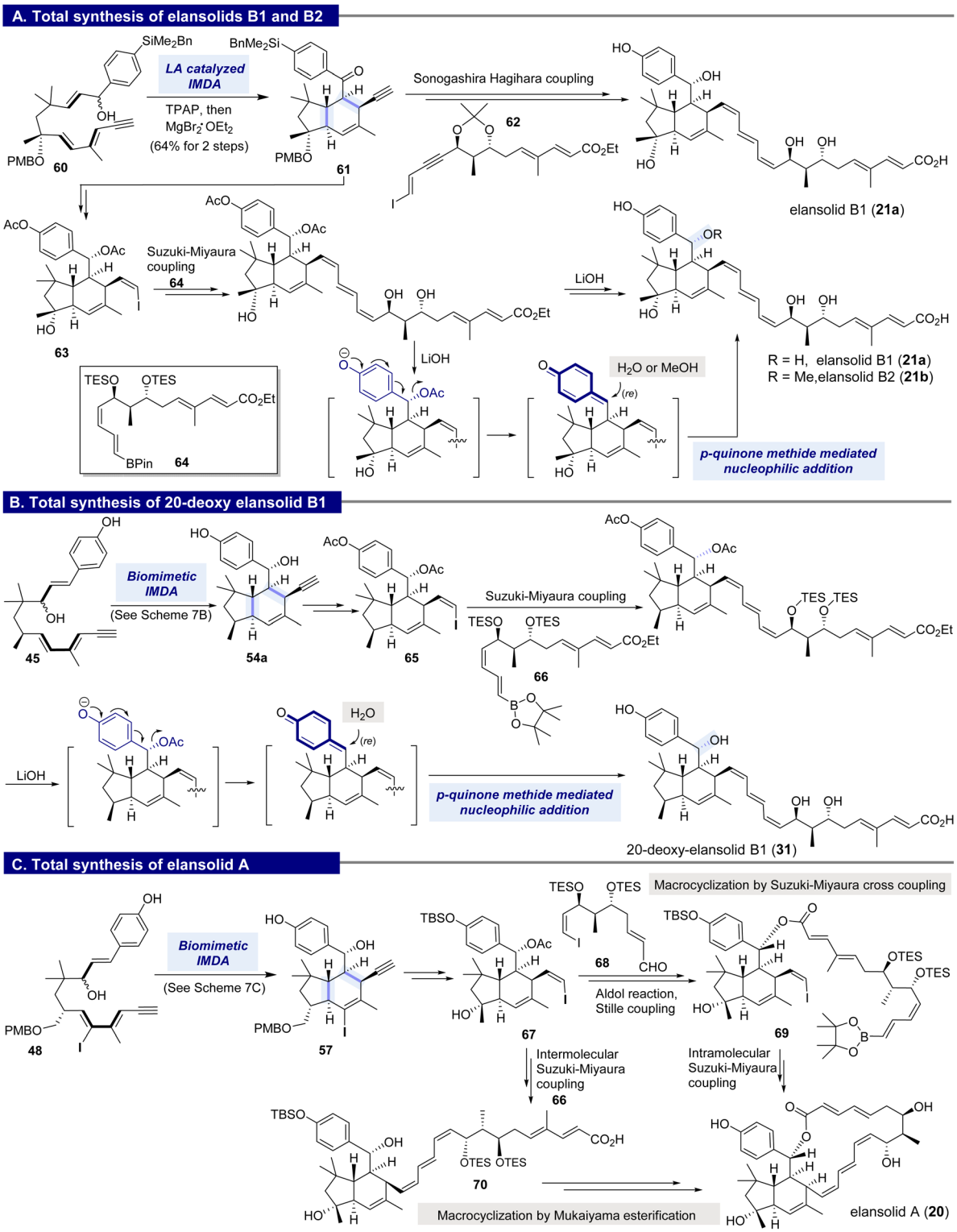

Scheme 9 Biomimetic total synthesis of various elansolids *via* *p*-quinone methide intermediates. (A) Total synthesis of elansolid B1 (**21a**) and elansolid B2 (**21b**); (B) total synthesis of 20-deoxy elansolid B1 (**31**); (C) total synthesis of elansolid A (**20**). The biomimetic steps are highlighted in light blue.

well suited for the generation of a vinylogous quinone methide intermediate and hence, yielded the two diastereomeric tertrahydroindanes **56a** and **56b**. Still, facial selectivity was poor (Scheme 8C, central right).[31]

It was rationalised that the low facial selectivities observed for the different IMDA cycloadditions from *p*-quinone methides generated *in situ* could be overcome by hampering the free rotation around the C19–C20 bond in the precursor substrates.

Therefore, precursor **48** was designed, which shows restricted conformational flexibility. For this purpose, iodine was chosen to serve as a large substituent at C18. This structural scenario brings the stereocenter at C20 into play as a substrate-based directing chiral center. Compound **48** contains an additional OPMB group, which could later be utilised to introduce the hydroxyl group at C20. In the "fixed" conformation of the diene moiety, the iodine atom and the hydrogen atom at position C20 are oriented in the same direction in a coplanar manner to minimise the 1,3-allylic strain.[32] Thus, the (*si*, *re*)-face of the diene moiety is ideally exposed to the vinylic *p*-methide quinone group. Under acidic conditions (Brønsted acid Tf_2NH at −40 °C), **48** yielded the desired IMDA product **57** as a single diastereomer, as confirmed by X-ray analysis (Scheme 8C, bottom right).[32] In accordance with the biosynthetic proposal, the vinylogous elimination of water takes place first to form the intermediate quinone methide **58**. Favored by the 1,3-allylic strain[33] induced by the "dummy" substituent iodine, the vinylic quinone methide becomes oriented above the diene unit. The subsequent IMDA cycloaddition yields the new *p*-quinone methide **59**, and after Michael addition of water from the less hindered (*re*)-face, tetrahydroindane **57** is formed.

It should be noted that the key enzyme in the PKS reaction pathway responsible for the IMDA catalyzes this reaction under complete conformational control (Scheme 4). It can be assumed that the linear precursor bound to the ACP of module **10** already adopts the conformation required for IMDA before the dehydration step occurs. Thus, the resulting vinylquinone methide is well positioned to approach the diene moiety from the face that leads to the IMDA product in stereochemical terms. In the course of evolution, nature thus developed biocatalysts with ever-increasing catalytic efficiency, and this evolutionary process also involved a pronounced "folding ability." This is clearly demonstrated in the present example, but applies even more strongly to terpene synthases and the formation of (oligo) cyclic terpenoids.[34] Chemists can and should learn from the synthetic chemist Mother Nature,[35] not only regarding catalyst design but also in the development of sophisticated chemical approaches to mimic enzyme function, as illustrated in Scheme 8C (bottom right).

3.3 Total syntheses of elansolids utilizing *p*-methide quinone intermediates

The validation of the biosynthetic proposal paved the way for the finalisation of the total syntheses of various elansolids. In particular, total synthesis approaches to elansolids A (**20**), B1 (**21a**), and B2 (**21b**), along with 20-deoxy elansolid B1 (**31**), were achieved. These syntheses and the key intermediates are briefly summarised in Scheme 9.

The first synthesis of elansolid B1 (**21a**) differed from the other IMDA methods in that allyl alcohol **60** was first oxidised to the corresponding enone, which could then be converted to tetrahydroindane **61** with excellent selectivity ($dr = 30:1$) in the presence of a Lewis acid catalyst (Scheme 9A).[36] Note that in this case, a silyl group was present at the site of the phenolic hydroxy group, which was later converted to the phenol under Tamao–Fleming conditions.[37] The ketone in **61** served as the starting point for two different routes to elansolid B1 **21a**, which commenced with the reduction of the ketone by $LiAlH_4$ with moderate diastereocontrol ($dr = 3:1$). In the first case, a Sonogashira–Hagihara reaction with the C1–C12 polyketide fragment **62** served as the key step to fully assemble the carbon backbone of the elansolids. Functional group manipulations then provided the target elansolid B1 (**21a**). The alternative route also relied on tetrahydroindanone **61**,[38] which was transformed into vinyl iodide **63** by ketone reduction and alkyne iodination, followed by *syn*-hydrogenation, as the key steps.[39] The carbon backbone was fully assembled by a Suzuki–Miyaura cross-coupling reaction with fragment **64**. In the final step, the benzylic acetate group was cleaved under basic conditions to form the *p*-quinone methide, which was then attacked stereoselectively by water or methanol. This yielded elansolids B1 (**21a**) and B2 (**21b**).

The unnatural 20-deoxy-elansolid B1 (**31**) was also prepared by following this synthetic strategy. This new derivative within the elansolid family could be used to test whether the hydroxy group introduced at C20 by the final step of the biosynthesis is relevant for the antibiotic property of elansolids (Scheme 9B).[26] Tetrahydroindane **54a** (obtained by the biomimetic IMDA cycloaddition from **45**) served as the starting point from where vinyl iodide **65** was prepared. This was reacted with vinyl boronic acid diester **66** under cross-coupling conditions. The resulting product was further processed to 20-deoxy elansolid B1 (**31**), and it was found that it exerted similar antibacterial properties to elansolid A2 (**20***). This finding demonstrates that the alcohol at C20 does not significantly influence the bioactivity of the elansolids.

Finally, the macrocyclic elansolid A (**20**) was synthesised by converting the linear precursor **48** into the iodine-modified tetrahydroindane **57** using the iodine-based "dummy" trick, which was then further converted into vinyl iodide **67**.[32] From here, two alternative routes to elansolid A were pursued. One route first connects the polyketide chain to C25, and macrocyclisation is achieved by intramolecular Suzuki cross-coupling chemistry (Scheme 9C).[40] To achieve this, the acetate group at C25 was utilised for an aldol coupling with aldehyde **68**, thereby incorporating the missing carbon atoms. The vinyl iodide was homologated to vinyl boronate **69** using Stille coupling chemistry,[41] which then served to carry out the intramolecular Suzuki cross-coupling and thus ring closure, ultimately leading to elansolid A (**20**).

Alternatively, macrolactonisation could also be realised by an intramolecular Mukaiyama esterification reaction[42] of carboxylic acid **70** that finally provided elansolid A (**20**).

As shown in Scheme 9, it is worth noting that, based on the established Suzuki–Miyaura coupling method and the macrolactonization protocol, simplified analogs of elansolid A1/A2 can also be prepared, in which the cyclopentane group has been removed while the macrolactone ring has been retained.[43]

4. Conclusion

Due to their high reactivity, unhindered *p*-quinone methides pose a particular challenge in synthetic chemistry. However,

these structural elements are found in various bioactive natural products such as celastrol and pristimerin, 20-*epi*-isoiguesterinol, tingenone, taxodone, taxodione, kendomycin, elansolid A3, *etc.* Evidently, in the course of evolution, nature has developed ways and methods to generate these species, use them as intermediates, or preserve them as structural elements in secondary metabolites. A deeper understanding of "Nature's knowledge" can serve as a starting point for the development of chemical methods and synthetic strategies.

Elansolid A3 can be considered a perfect "telling example". The biosynthesis of elansolid A3 suggests that the dehydratase is most likely responsible for the allylic dehydration step that leads to the formation of the vinyl-*p*-quinone methide intermediate in the PKS assembly line, which triggers the subsequent IMDA cyclisation and provides the central tetrahydroindane skeleton.

Inspired by this biosynthesis proposal, the total syntheses of various elansolids were accomplished, which on the one hand confirmed the correctness of the biosynthesis proposal and on the other hand led to the discovery of a new cascade reaction involving the formation of *p*-quinone methide intermediates, followed by the *in situ* utilisation of these species in a Diels–Alder cycloaddition. The synthetic work also indicates why, from a biosynthetic point of view, oxidation at C20 only occurs after the formation of the tetrahydroindane skeleton, precisely because of the complexity of stereochemical control in the context of cycloaddition.

Elansolid A3 can be regarded as a raw model, demonstrating that when biosynthesis and chemical synthesis enter into a close symbiosis, new chemical insights and methods can be gained, as presented here on the subject of the chemistry of *p*-quinone methides.

Future lines of research will undoubtedly focus on the localisation, characterisation, expression and functional analysis of the enzymes responsible for the cascade reaction described. It may well be that this is merely a modified hydratase that initiates the vinylogic elimination of water and, in doing so, conformationally aligns the vinylquinone methide in such a way that a 'chemical' spontaneous IMDA reaction can take place, whilst also controlling the facial selectivity. The main hurdle here is its integration as a module within the architecture of the polyketide synthase. Individual modules are difficult to study in isolation within such megaenzyme complexes. However, elucidating the mechanism of this unusual key step would also benefit synthetic chemistry, just as nature has repeatedly inspired synthetic chemists in the field of natural product synthesis and methodological development.[35,44]

It would make sense to further develop the most active elansolid derivatives in medicinal chemistry programmes, whereby biotechnological and hybrid methods such as mutasynthesis[45] could also be considered.

5. Author contributions

L.-L. W. wrote the first draft and reviewed as well as edited the manuscript. X.-Q. Z. carried out the validation. AK wrote, reviewed and edited the manuscript and was responsible for the graphical design.

6. Conflicts of interest

There are no conflicts to declare.

7. Data availability

No supporting data come along with this article.

8. Acknowledgements

This work was financially supported by the Strategic Priority Research Program of the Chinese Academy of Sciences (CAS) (XDB1230202), the Research Program of the Lingang Laboratory (LGL-2612-19), the Strategic Priority Research Program of the Kunming Institute of Botany, CAS (KIBXD202402), the Yunnan Fundamental Research Projects (202401AS070096), the CAS "Light of West China" Program for Young Scholars in Regional Development, and the CAS Interdisciplinary Team of "Light of West China" Program (xbzg-zdsys-202405). The work was funded in part by the Studienstiftung des Deutschen Volkes who provided a scholarship to Richard Dehn (see ref. 18, 19, 24 and 30).

9. References

1 (*a*) L.-N. Gao, K. Zheng, H.-Y. Chen, Y.-N. Gao, Z.-Z. Li, C. He, S.-H. Huang, R. Hong, M. Bian and Z.-J. Liu, *Org. Biomol. Chem.*, 2025, **23**, 2775–2792; (*b*) T. N. Purdy, B. S. Moore and A. L. Lukowski, *J. Nat. Prod.*, 2022, **85**, 688–701; (*c*) N. J. Willis and C. D. Bray, *Chem.–Eur. J.*, 2012, **18**, 9160–9173; (*d*) W.-J. Bai, J. G. David, Z.-G. Feng, M. G. Weaver, K.-L. Wu and T. R. R. Pettus, *Acc. Chem. Res.*, 2014, **47**, 3655–3664; (*e*) W. Li, X. Xu, P. Zhang and P. Li, *Chem.–Asian J.*, 2018, **13**, 2350–2359; (*f*) J. L. Bolton and J. A. Thompson, Formation and Reactions of Xenobiotic Quinone Methides in Biology, in *Reactive Intermediates in Chemistry and Biology: Quinone Methides*, ed. S. E. Rokita, Wiley, 2009, pp. 329–356.

2 (*a*) J.-Y. Wang, W.-J. Hao, S.-J. Tu and B. Jiang, *Org. Chem. Front.*, 2020, **7**, 1743–1778; (*b*) C. G. S. Lima, F. P. Pauli, D. C. S. Costa, A. S. de Souza, L. S. M. Forezi, V. F. Ferreira and F. D. C. D. Silva, *Eur. J. Org Chem.*, 2020, 2650–2692.

3 S. B. Cavitt, R. H. Sarrafizadeh and P. D. Gardner, *J. Org. Chem.*, 1962, **7**, 1211–1216.

4 J. Gao, Q. Chen and Q. Zhang, *Nat. Prod. Rep.*, 2025, **42**, 1676–1689.

5 A. A. L. Gunatilaka, *Triterpenoid Quinonemethide and Related Compounds*, Springer-Verlag, Wien, Austria, 1996.

6 D. A. Thiem, A. T. Sneden, S. I. Khan and B. L. Tekwani, *J. Nat. Prod.*, 2005, **68**, 251–254.

7 H. Chavez, A. Estevez-Braun, A. G. Ravelo and A. G. Gonzalez, *J. Nat. Prod.*, 1999, **62**, 434–436.

8 W. N. Setzer, M. T. Holland, C. A. Bozeman, G. F. Rozmus, M. C. Setzer, D. M. Moriarity, S. Reeb, B. Vogler, R. B. Bates and W. A. Haber, *Planta Med.*, 2001, **67**, 65–69.
9 S. M. Kupchan, A. Karim and C. Marcks, *J. Am. Chem. Soc.*, 1968, **90**, 5923–5924.
10 H. B. Bode and A. Zeeck, *J. Chem. Soc., Perkin Trans. 1*, 2000, **323**, 323–328.
11 R. Jansen, K. Gerth, H. Steinmetz, S. Reinecke, W. Kessler, A. Kirschning and R. Müller, *Chem.–Eur. J.*, 2011, **17**, 7739–7744.
12 (*a*) A. M. Zaghloul, A. A. Gohar, Z. A. Naiem and F. M. A. Bar, *Z. Naturforsch., C:J. Biosci.*, 2008, **63**, 355–360; (*b*) A. Ulubelen, G. Topçu, H.-B. Chai and J. M. Pezzuto, *Pharm. Biol.*, 1999, **37**, 148–151.
13 U. Kolak, A. Kabouche, M. Öztürk, Z. Kabouche, G. Topçu and A. Ulubelen, *Phytochem. Anal.*, 2009, **20**, 320–327.
14 (*a*) V. K. Bajpai and S. C. Kan, *J. Biosci.*, 2010, **35**, 533–538; (*b*) V. K. Bajpai, M. Na and S. C. Kang, *Food Chem. Toxicol.*, 2010, **48**, 1945–1949; (*c*) M. Tada, J. Kurabe, T. Yoshida, T. Ohkanda and Y. Matsumoto, *Chem. Pharm. Bull.*, 2010, **58**, 818–824; (*d*) N. Kusumoto, T. Ashitani, T. Murayama, K. Ogiyama and K. Takahashi, *J. Chem. Ecol.*, 2010, **36**, 1381–1386; (*e*) N. Kusumoto, T. Ashitani, Y. Hayasaka, T. Murayama, K. Ogiyama and K. Takahashi, *J. Chem. Ecol.*, 2009, **35**, 635–642; (*f*) M. C. Ballesta-Acosta, M. J. Pascual-Villalobos and B. Rodríguez, *Spanish J. Agric. Res.*, 2008, **6**, 85–91.
15 F. Dufrasne, M. Gelbcke, J. Nève, R. Kiss and J.-L. Kraus, *Curr. Med. Chem.*, 2011, **18**, 3995–4011.
16 J. L. Bolton, *Curr. Org. Chem.*, 2014, **18**, 61–69.
17 K. Gerth, H. Steinmetz and G. Höfle, Elansolids, Novel Natural Metabolites of Flexibacter and Antibiotically Active Derivatives thereof, EP 2093212A1, 2009.
18 H. Steinmetz, K. Gerth, R. Jansen, N. Schläger, R. Dehn, S. Reinecke, A. Kirschning and R. Müller, *Angew. Chem., Int. Ed.*, 2011, **50**, 532–536.
19 H. Steinmetz, W. Zander, M. A. M. Shushni, R. Jansen, K. Gerth, R. Dehn, G. Dräger, A. Kirschning and R. Müller, *ChemBioChem*, 2012, **13**, 1813–1817.
20 An oxygenated elansolid type of macrolides isolated from marine heterotrophic bacterium B. amyloliquefaciens MTCC 12716 was reported by Chakraborty and co-workers. see: V. K. Kizhakkekalam, K. Chakraborty and M. Joy, *Int. J. Antimicrob. Agents*, 2020, **55**, 105892.
21 S. D. Rychnovsky and D. J. Skalitxky, *Tetrahedron Lett.*, 1990, **31**, 945–948.
22 D. A. Evans, D. L. Rieger and J. R. Gage, *Tetrahedron Lett.*, 1990, **31**, 7099–7100.
23 R. H. Grubbs, *Tetrahedron*, 2004, **60**, 7117–7140.
24 (*a*) D. E. Cane, F. Kudo, K. Kinoshita and C. Khosla, *Chem. Biol.*, 2002, **9**, 131–142; (*b*) A. Kirschning, F. Taft and T. Knobloch, *Org. Biomol. Chem.*, 2007, **5**, 3245–3259.
25 A. Beckmann, S. Hüttel, V. Schmitt, R. Müller and M. Stadler, *Microb. Cell Fact.*, 2017, **16**, 143.
26 L.-L. Wang, D. Candito, G. Dräger, J. Herrmann, R. Müller and A. Kirschning, *Chem.–Eur. J.*, 2017, **23**, 5291–5298.
27 R. Dehn, Y. Katsuyama, A. Weber, K. Gerth, R. Jansen, H. Steinmetz, G. Höfle, R. Müller and A. Kirschning, *Angew. Chem., Int. Ed.*, 2011, **50**, 3882–3887.
28 R. Teta, M. Gurgui, E. J. N. Helfrich, S. Künne, A. Schneider, G. V. Echten-Deckert, A. Mangoni and J. Piel, *ChemBioChem*, 2010, **11**, 2506–2512.
29 H. Oikawa and T. Tokiwano, *Nat. Prod. Rep.*, 2004, **21**, 321–352.
30 L.-L. Wang, D. Candito, G. Dräger and A. Kirschning, *Eur. J. Org Chem.*, 2017, 5582–5591.
31 Q. Yu, S. Yang, C. Tang, L. Peng, Z. Zuo and L.-L. Wang, *Chin. J. Org. Chem.*, 2021, **41**, 2820–2830.
32 L.-L. Wang, Q. Yu, W. Zhang, S. Yang, L. Peng, L. Zhang, X.-N. Li, F. Gagosz and A. Kirschning, *J. Am. Chem. Soc.*, 2022, **144**, 6871–6881.
33 R. W. Hoffmann, *Chem. Rev.*, 1989, **89**, 1841–1860.
34 V. Harms, A. Kirschning and J. S. Dickschat, *Nat. Prod. Rep.*, 2020, **37**, 1080–1097.
35 G. Jürjens, A. Kirschning and D. Candito, *Nat. Prod. Rep.*, 2015, **32**, 723–737.
36 A. Weber, R. Dehn, N. Schläger, B. Dieter and A. Kirschning, *Org. Lett.*, 2014, **16**, 568–571.
37 (*a*) K. Tamao, T. Kakui, M. Akita, T. Iwahara, R. Kanatani, J. Yoshida and M. Kumada, *Tetrahedron*, 1983, **39**, 983–990; (*b*) I. Fleming, R. Henning and H. J. Plaut, *J. Chem. Soc., Chem. Commun.*, 1984, 29–31.
38 L.-L. Wang and A. Kirschning, *Beilstein J. Org. Chem.*, 2017, **13**, 1280–1287.
39 O. Hartmann and M. Kalesse, *Org. Lett.*, 2012, **14**, 3064–3067.
40 N. Miyaura and A. Suzuki, *J. Chem. Soc., Chem. Commun.*, 1979, 866–867.
41 J. K. Stille and B. L. Groh, *J. Am. Chem. Soc.*, 1987, **109**, 813–817.
42 K. Narasaka, K. Maruyama and T. Mukaiyama, *Chem. Lett.*, 1978, 885–888.
43 S. Yang, J. Wu and L.-L. Wang, *Chin. J. Org. Chem.*, 2024, **44**, 2350–2362.
44 A. Kirschning and F. Hahn, *Angew. Chem., Int. Ed.*, 2012, **51**, 4012–4022.
45 (*a*) D. J. Vollmann, L. Winand and M. Nett, *Curr. Opin. Biotechnol.*, 2022, **77**, 102761; (*b*) P. Groverorcid, D. K. Sharma, A. K. Chhalodia and D. Mukherjee, *Curr. Org. Chem.*, 2021, **25**, 1611–1625; (*c*) J. Kennedy, *Nat. Prod. Rep.*, 2008, **25**, 25–34; (*d*) S. Weist and R. D. Süssmuth, *Appl. Microbiol. Biotechnol.*, 2005, **68**, 141–150.